The State of the Molecular Gas in M 82

A. Weiß[1], N. Neininger[1], S. Hüttemeister[1], U. Klein[1]

[1]Radioastronomisches Institut Univ. Bonn, Auf dem Hügel 71, D-53121 Bonn, Germany

Abstract

We present the results of a high–angular resolution CO analysis of the molecular gas in M 82. Radiative transfer calculations suggest that the kinetic gas temperature and density of the CO emitting volume change across the starburst nucleus. A detailed analysis of the conversion factor from CO intensity to H_2 column density shows that X_{CO} depends on the excitation conditions. We discuss evidence for cloud evaporation at the starburst center.

1 Observations

We have used the PdBI to observe the $^{12}CO(J=2 \rightarrow 1)$ and $C^{18}O(J=1 \rightarrow 0)$ emission lines in the central region of M 82. The spatial resolution was $3.8'' \times 3.5''$ at 109 GHz and $1.5'' \times 1.4''$ at 230 GHz. In addition to the high–resolution CO data we observed the $^{12}CO(J=1 \rightarrow 0)$, $^{12}CO(J=2 \rightarrow 1)$ and $^{13}CO(J=1 \rightarrow 0)$ emission lines with the IRAM 30m telescope in the on–the–fly mode. To ensure that the interferometric line intensities do not suffer from missing flux due to extended emission we combined the interferometer and the single–dish data cubes. For details see Weiß et al. (2001).

2 CO and tracers of ongoing star formation in M 82

The CO distribution in M 82 has been studied by several authors over the last few years. Fig. 1 show the integrated $^{12}CO(J=2 \rightarrow 1)$ line intensities observed with the Plateau de Bure Interferometer (PdBI) (Weiß et al. 2001). The overall morphology is very similar to the $^{12}CO(J=1 \rightarrow 0)$ distribution published by Shen & Lo (1995) and the $^{13}CO(J=1 \rightarrow 0)$ distribution published by Neininger et al. (1998). It shows a triple peak morphology of which the two outer lobes have been interpreted as the edge of a central molecular toroid (Nakai et al. 1987, Shen & Lo 1995), and a weaker central peak located 65 pc west of the M 82's center (2.2μm peak; Dietz et al. 1986). Most tracers of star formation in M 82 indicate that the highest star–forming activity is not associated with the molecular peaks which presumably indicate the location of the reservoirs for the 'fuel' for star formation but rather takes place between the peaks. The high–resolution 12.4 μm image of the central region of M 82 published by Telesco & Gezari (1992) suggests that the young stellar clusters, which heat the dust, are located between the western molecular lobe and the 2.2 μm nucleus (western mid infrared (MIR) peaks), at the central CO peak, and between the central CO peak and the eastern CO lobe (eastern MIR peak). A similar morphology is visible in the NeII line emission (Achtermann & Lacy 1995). The radio continuum point sources, which are believed to be supernova remnants (SNR) and compact HII regions, are spread across a much wider region and seem to avoid MIR and NeII peaks (Kronberg et al. 1985). Only the strongest SNR in M 82, SNR41.9+58, appears to be related to features at other wavelengths: it is located near the center of the expanding molecular superbubble, between the central and western CO peak, from which hot X–ray emitting gas is released into the halo of M 82 (Weiß et al. 1999).

"Dwarf Galaxies and their Environment"; Bad Honnef, Germany, 23-27 January 2001; Eds. K.S. de Boer, R.-J.Dettmar, U. Klein; Shaker Verlag

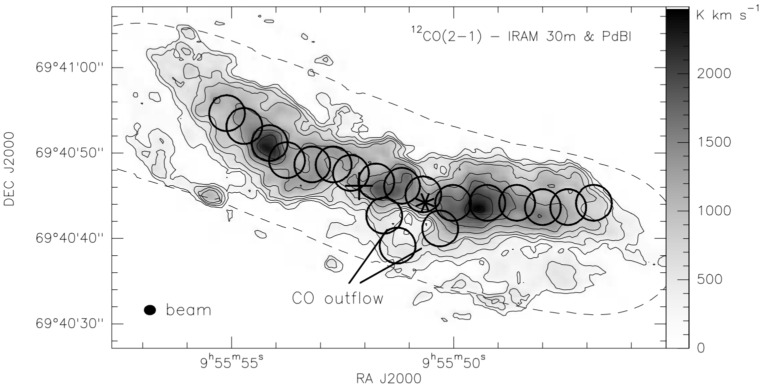

Figure 1: Integrated ^{12}CO($J = 2 \rightarrow 1$) line intensity derived from the short–spacing corrected data cube. The cross indicates the center of M 82 (2.2μm peak), the star represents the location of the brightest radio continuum point source (SNR 41.9+58) in M 82. Circles indicate the positions and resolution for which the LVG models have been calculated. The dotted line shows the 50% sensitivity level of the primary beam mosaic.

3 The state of the molecular gas in M 82's center

In order to address the question how the starburst influences the physical state of the molecular gas we calculated the physical conditions of the CO–emitting volume using a spherical, isothermal one–component large velocity gradient (LVG) model (de Jong et al. 1975, Henkel et al. 1980). Using our observations in conjunction with the high–resolution observations of the ^{12}CO($J = 1 \rightarrow 0$) transition (Shen & Lo 1995) and the ^{13}CO($J = 1 \rightarrow 0$) transition (Neininger et al. 1998) we have analyzed 19 positions across the major axis of M 82; for details see Weiß et al. (2001). The calculations show that the kinetic temperature is well correlated with the MIR emission and other tracers of high–level star formation. Within the prominent CO lobes with less signs of ongoing star formation, the kinetic temperature is about 50 K. Towards the active star–forming regions we find two kinetic temperature peaks above 150 K. These 'hot–spots' coincide with the location of MIR peaks (for a comparison between the MIR emission and the CO distribution see Telesco & Gezari 1992). Near the 2.2μm nucleus the LVG models suggest temperatures of about 75 K. H_2 densities are high in regions with low kinetic temperatures and vice versa. The solutions for the outer CO lobes suggest an H_2 density of $n(H_2) \approx 10^{4.0}$cm^{-3} with a tendency towards somewhat lower values at the very edge of the CO distribution ($n(H_2) \approx 10^{3.5}$cm^{-3}). At the 'hot–spot', low H_2 densities of $n(H_2) = 10^{2.8-3.1}$cm^{-3} are required to match the observed line ratios. Thus the CO emission in the active regions arises mainly from a warm, diffuse gas component, while in the outer parts the emission comes from a cold, dense environment.

4 Conversion from CO intensity to H_2 column density (X_{CO})

In order to derive the conversion factor between I(CO) and $N(H_2)$ (X_{CO}) we have calculated the H_2 column density at each analysed position from the results of our LVG models and under the assumption of LTE (for details see Weiß et al. 2001). The calculations clearly show that most of the molecular gas traced by CO is located in the outer CO lobes. The central 300 pc between the molecular lobes contain only about 20–30% of the molecular gas mass. This is in contradiction to what one would derive using the CO distribution as a tracer of H_2 column density. This implies that X_{CO} is *not* constant across the nucleus of M 82. The variation of the conversion factor X_{CO} with position is shown in Fig. 2, left. Note that X_{CO} is lower than the Galactic value of 1.6×10^{20} cm^{-2} (K km s^{-1})$^{-1}$ (Hunter et al. 1997) at all positions and for both methods. We find that X_{CO} varies across the disk of M 82 by about a factor of 5 if one considers the LTE solutions, and by a factor of 8 for the LVG solutions ($X_{CO} = 1.3 - 11.5 \times 10^{19}$ cm^{-2} (K km s^{-1})$^{-1}$). Both methods

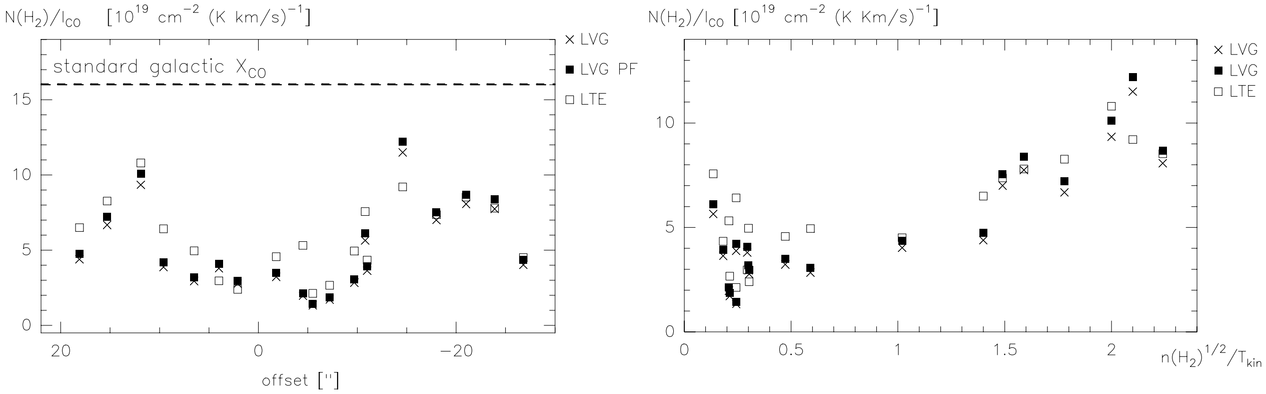

Figure 2: *Left:* Variation of $X_{\rm CO}$ across the analyzed positions in M 82. Offsets are given relative to the center of M 82 (2.2μm peak). The H_2 column densities were derived using the LTE, the LVG and LVG$_{PF}$ solutions. For the definition of LVG and LVG$_{PF}$ solutions see Weiß et al. (2001). The dotted line at $X_{\rm CO} = 1.6\times10^{20}\,{\rm cm^{-2}\,(K\,km\,s^{-1})^{-1}}$ corresponds to the standard Galactic conversion factor. *Right:* $X_{\rm CO}$ as derived from the LTE, LVG and LVG$_{PF}$ solutions versus $T_{\rm kin}^{-1}\,n({\rm H_2})^{1/2}$. The plot shows a linear correlation between the conversion factor and the associated H_2 densities and kinetic temperatures beyond $T_{\rm kin}^{-1}\,n({\rm H_2})^{1/2} \approx 0.5$.

show that the lowest conversion factors are associated with the central star–forming regions where the gas is heated by UV photons from the newly formed stars and cosmic–rays from SNRs. The CO–emitting volume at these positions has high kinetic temperatures. Towards the outer molecular lobes with higher H_2 densities and lower kinetic temperatures, the conversion factor rises. This is in agreement with simple theoretical arguments that suggest that the conversion factor $X_{\rm CO}$ should be proportional to $T_{\rm kin}^{-1}\,n({\rm H_2})^{1/2}$ for virialized clouds (Maloney & Black 1988). The variation of $X_{\rm CO}$ with $T_{\rm kin}^{-1}\,n({\rm H_2})^{1/2}$ is shown in Fig. 2, right. The linear correlation between $X_{\rm CO}$ and $T_{\rm kin}^{-1}\,n({\rm H_2})^{1/2}$ for $T_{\rm kin}^{-1}\,n({\rm H_2})^{1/2} > 0.5$ is clearly visible. For $T_{\rm kin}^{-1}\,n({\rm H_2})^{1/2} < 0.5$ the scatter in the plot increases. This is in particular true for $X_{\rm CO}$ calculated under the assumption of LTE. This suggests that the gas is not close to LTE at the 'hot spots'. The increased scatter of $X_{\rm CO}$ calculated with the LVG method might suggest that either the clouds are not virialized or that more appropriate models (like PDR models) are required to calculate the physical gas properties in the center of the starburst.

5 Cloud stability in the starburst nucleus

The existence of a low density H_2 component in the nuclear region of M 82 raises the question how it can survive under the extreme condition in the starburst nucleus. From the strength of the observed UV field one would expect that clouds with densities less than $10^4\,{\rm cm^{-3}}$ cannot exist in M 82's center (Brouillet & Schilke 1993). In addition, such a gas component is barely dense enough to avoid tidal disruption (Mao et al. 2000), which would support a rather diffuse distribution of the gas. To emphasize this point we have plotted the H_2 densities derived from our LVG solutions versus the distance from M 82's center in a stability diagram (Fig. 3). For the minimum density required to achieve stability as a function of radius (solid line), we have assumed a mass distribution of the stars of $M(r) \propto r^{1.2}$ and a typical cloud size of 1 pc (Weiß et al. 2001). While the gravity of the dense gas in the molecular lobes is clearly capable to compensate tidal forces, the low–density H_2 component near the nucleus has densities near or below the minimum density. As a consequence, this would imply that these clouds are not virialized. This could explain why the linear correlation between $T_{\rm kin}^{-1}\,n({\rm H_2})^{1/2}$ and $X_{\rm CO}$ is not valid for $T_{\rm kin}^{-1}\,n({\rm H_2})^{1/2} < 0.5$, hence for the warm and low–density gas in the starburst center (see circles in the Fig. 3). Such a scenario would explain the

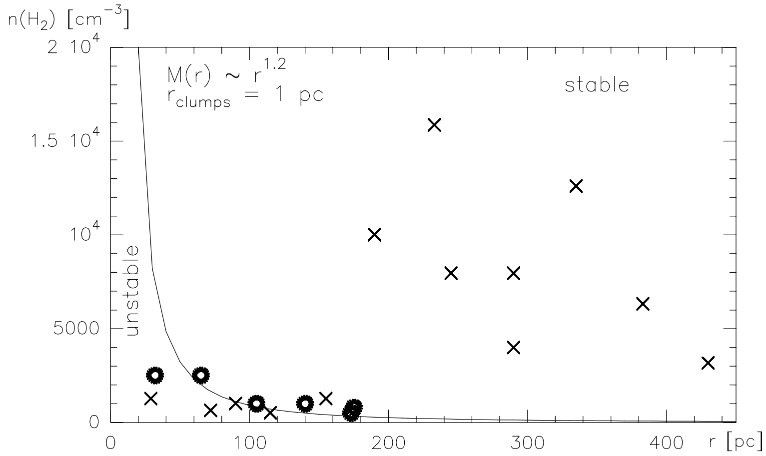

Figure 3: Density of molecular clouds at a given distance from the center of M 82, which is required to achieve stability against tidal forces. The solid line indicates the minimum density required to achieve stability. The markers indicate the LVG densities for the analysed positions. The positions indicated by the circles are those which do not follow the linear correlation in Fig. 2 (right).

high [CI]/[CO] abundance ratios observed in M 82 (Schilke et al. 1993; White et al. 1994) and the depletion of H_2 in the central 300 pc of M 82. Nevertheless, the stability argument for the clouds disregards other forces like an additional support of the clouds by overpressure of the surrounding medium. In fact, FIR spectroscopy of H II regions in M 82 has shown that their pressure is of order $P/k \approx 2 \times 10^6\,\mathrm{K\,cm^{-3}}$ (Duffy et al. 1987). Similarly high values have been derived from PDR models for molecular cloud surfaces in the starburst nucleus (Lord et al. 1996). These values are a magnitude higher than the pressure of the cold molecular phase. Thus the pressure of the ambient medium stabilizes the molecular clouds and might explain why molecular gas is still capable to survive in the nucleus of M 82. Nevertheless, more detailed numerical analyses of evaporation time scales and related questions are needed to settle this question.

References

Achtermann J.M., Lacy J.H., 1995, ApJ 439, 163
Brouillet N., Schilke P., 1993, A&A 277, 381
de Jong T., Chu S.I., Dalgarno A., 1975, ApJ 199, 69
Dietz K., Smith J., Hackwell J.A., Gehrz D.R., Grasdalen G.L., 1986, AJ 91, 758
Duffy, Pl.B., Erickson, E.F., Haas, M.R., Houck, J.R., 1987, ApJ 315, 68
Henkel, C., Walmsley, C.M., Wilson, T.L., 1980, A&A 82, 41
Hunter S.D., Bertsch D.L., Catelli J.R., et al., 1997, ApJ 481, 205
Kronberg P.P., Biermann P., Schwab F.R., 1985, ApJ 291, 693
Lord, S., Hollenbach, D.,J., Haas, M.R., et al., 1996, ApJ, 465, 703
Maloney P., Black J.H., 1988, ApJ 325, 389
Mao R.Q., Henkel C., Schulz A., et al. , 2000, A&A 358, 433
Neininger N., Guèlin M., Klein U., García-Burillo S., Wielebinski R., 1998, A&A 339, 737
Schilke P., Carlstrom J.E., Keene J., Phillips T.G., 1993, ApJ 417, L97
Shen J., Lo K.Y., 1995, ApJ 445, L99
Nakai N., Hayashi M., Handa T., Sofue Y., Hasegawa T., 1987, PASJ 39, 685
Telesco C.M., Gezari D.Y., 1992, ApJ 395, 461
Weiß A., Neininger, N., Hüttemeister, S., Klein, U., 2001, A&A 365, 571
Weiß A., Walter F., Neininger N., Klein U., 1999, A&A 345, L23
White G.J., Ellison B., Claude S., Dent W.R.F., Matheson D.N., 1994, A&A 284, L23